Acta Mech 219, 129–143 (2011)
DOI 10.1007/s00707-011-0445-7

Yasuhide Shindo · Fumio Narita · Takuya Matsuda

Electric field dependence of the mode I energy release rate in single-edge cracked piezoelectric ceramics: effect due to polarization switching/dielectric breakdown

Received: 11 November 2010 / Published online: 30 January 2011

Abstract This study presents the results of the mode I energy release rate of a rectangular piezoelectric material with a single-edge crack under electromechanical loading. A crack was created normal or parallel to the poling direction, and electric fields were applied parallel and antiparallel to the poling. A nonlinear plane strain finite element analysis was carried out, and the effect of localized polarization switching on the energy release rate was discussed for the permeable, impermeable, open, and discharging cracks under a high-negative electric field. The effect of dielectric breakdown on the energy release rate was also examined under a high-positive electric field.

1 Introduction

Piezoelectric lead zirconate titanate (PZT) ceramics have become very popular in sensor and actuator components of smart materials and structures. To be successful in such device applications, piezoelectric ceramics must provide adequate reliability and durability under severe electromechanical loading conditions. Successful designs require comprehensive evaluation of crack behavior in piezoelectric ceramics, and fully understanding of the piezoelectric fracture mechanics parameters such as the energy release rate is of great importance. Over the past two decades, there has been controversy about the electrical boundary conditions across the piezoelectric crack face. In the theoretical studies of the piezoelectric crack problems, three electrical boundary conditions across the crack face have commonly been used, i.e., the permeable crack [1,2], impermeable crack [3,4], and open piezoelectric crack [5] models. Zhao et al. [6] analyzed central and edge cracks in piezoelectric ceramic strips based on the permeable, impermeable, and open crack models, and discussed the stress and electric displacement intensity factors. Although the impermeable and open crack models may provide the mathematical solutions of the piezoelectric cracks, it is still questionable to use these models to search for fracture design parameters characterizing the electric failure. In recent years, a nonlinear electrically discharging crack model was proposed, and the effect of the electric breakdown field within the crack gap on the energy release rate of the piezoelectric ceramics was discussed [7]. Mode I stress and electric displacement were applied, and various levels of the discharge field within the crack gap were used. However, doubt remained as to whether these conditions would be suitable, that is, the electric displacement can usually not be applied, and most of the discharge levels are very high. In order to resolve the effect of the crack face electrical boundary condition on the piezoelectric fracture mechanics parameters, Shindo et al. [8] discussed the mode I energy release rate of the piezoelectric ceramics under electromechanical loading. They showed that in modeling cracks in piezoelectric ceramics the impermeable and open crack face assumptions can lead to an unphysical negative energy release rate under positive and negative electric fields and produce significant errors. They

Y. Shindo (✉) · F. Narita · T. Matsuda
Department of Materials Processing, Graduate School of Engineering,
Tohoku University, Aoba-yama 6-6-02, Sendai 980-8579, Japan
E-mail: shindo@material.tohoku.ac.jp

also found that, using the standard air breakdown field for a critical discharge level within the crack gap, the energy release rate for the discharging crack model becomes the energy release rate for the permeable crack model.

It is well known that under a high-negative electric field the nonlinear effect due to the polarization switching affects the piezoelectric crack behavior [9,10]. It is also expected that the fracture behavior of piezoelectric ceramics is influenced by the dielectric breakdown under a high-positive electric field [11]. Although a numerical method for the polarization saturation [12]/strip dielectric breakdown [13] model was proposed for cracked piezoelectric ceramics, the impermeable and open crack face assumptions and unrealistic loading conditions (very high applied stress and electric field/electric displacement) were used to calculate the energy release rate [14]. These unrealistic situations can be computed numerically, but the result is meaningless (i.e. the piezoelectric ceramics will fail under such conditions).

In this study, we examine the mode I energy release rate for a single-edge crack in a rectangular piezoelectric material under electromechanical loading. A crack was created normal or parallel to the poling direction, and electric fields were applied parallel and antiparallel to the poling. Many studies report the piezoelectric crack behavior based on the unrealistic model, whereas the present study treats the real situation. A nonlinear finite element analysis was employed to calculate the energy release rate for the plane strain permeable, impermeable, open, and discharging crack models. The effect of the applied electric field on the energy release rate was then discussed under various crack face electrical boundary conditions. The effects of localized polarization switching and dielectric breakdown on the energy release rate were also examined.

2 Finite element solution procedure

2.1 Problem statement and basic equations

Consider a rectangular piezoelectric material of length 2l and width h containing a single-edge crack of length a. The crack is assumed with faces normal (Case 1) or parallel (Case 2) to the polarization axis, as shown in Fig. 1. The origin of a Cartesian coordinate system (x, y, z) is located at the mouth of the crack. The piezoelectric material is under a state of plane strain in the y-direction and loaded by mechanical tension and electric field. Usually, the piezoelectric materials are driven by the poling direction of the electric field, and so we consider here the piezoelectric material subjected to an electric field parallel/antiparallel to the polarization axis. Because of symmetry, we need only to consider the upper half space region.

The governing equations are

$$\begin{aligned} \sigma_{xx,x} + \sigma_{zx,z} &= 0, \\ \sigma_{xz,x} + \sigma_{zz,z} &= 0, \end{aligned} \tag{1}$$

$$D_{x,x} + D_{z,z} = 0 \tag{2}$$

where $\sigma_{xx}, \sigma_{zz}, \sigma_{xz} = \sigma_{zx}$ are the components of the stress tensor, D_x and D_z are the components of the electric displacement vector, and a comma implies partial differentiation with respect to the coordinates. The

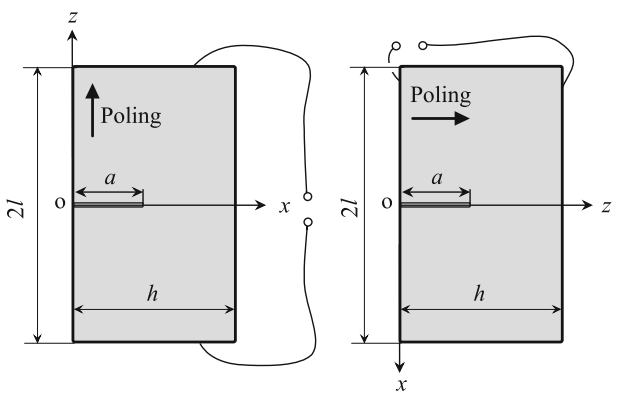

Fig. 1 A rectangular piezoelectric material with a single-edge crack: **a** Case 1; **b** Case 2

constitutive equations can be written as

$$\begin{Bmatrix} \sigma_{xx} \\ \sigma_{zz} \\ \sigma_{zx} \end{Bmatrix} = \begin{bmatrix} c_{11} & c_{13} & 0 \\ c_{13} & c_{33} & 0 \\ 0 & 0 & c_{44} \end{bmatrix} \begin{Bmatrix} \varepsilon_{xx} - \varepsilon_{xx}^{\mathrm{r}} \\ \varepsilon_{zz} - \varepsilon_{zz}^{\mathrm{r}} \\ 2(\varepsilon_{zx} - \varepsilon_{zx}^{\mathrm{r}}) \end{Bmatrix} - \begin{bmatrix} 0 & e_{31} \\ 0 & e_{33} \\ e_{15} & 0 \end{bmatrix} \begin{Bmatrix} E_x \\ E_z \end{Bmatrix}, \tag{3}$$

$$\begin{Bmatrix} D_x \\ D_z \end{Bmatrix} = \begin{bmatrix} 0 & 0 & e_{15} \\ e_{31} & e_{33} & 0 \end{bmatrix} \begin{Bmatrix} \varepsilon_{xx} - \varepsilon_{xx}^{\mathrm{r}} \\ \varepsilon_{zz} - \varepsilon_{zz}^{\mathrm{r}} \\ 2(\varepsilon_{zx} - \varepsilon_{zx}^{\mathrm{r}}) \end{Bmatrix} + \begin{bmatrix} \epsilon_{11} & 0 \\ 0 & \epsilon_{33} \end{bmatrix} \begin{Bmatrix} E_x \\ E_z \end{Bmatrix} + \begin{Bmatrix} P_x^{\mathrm{r}} \\ P_z^{\mathrm{r}} \end{Bmatrix} \tag{4}$$

where ε_{xx}, ε_{zz}, and ε_{zx} are the components of the strain tensor, E_x and E_z are the components of the electric field intensity vector, c_{11}, c_{13}, c_{33}, and c_{44} are the elastic stiffness constants, ϵ_{11} and ϵ_{33} are the dielectric permittivities, and e_{15}, e_{31}, and e_{33} are the piezoelectric constants. In Eqs. (3), (4), $\varepsilon_{xx}^{\mathrm{r}}$, $\varepsilon_{zz}^{\mathrm{r}}$, $\varepsilon_{zx}^{\mathrm{r}}$ and P_x^{r}, P_z^{r} are the components of remanent strains and polarizations, respectively. The strains can be written as

$$\varepsilon_{xx} = u_{x,x}, \quad \varepsilon_{zz} = u_{z,z}, \quad \varepsilon_{xz} = \varepsilon_{zx} = (u_{z,x} + u_{x,z})/2 \tag{5}$$

where u_x and u_z are the components of the displacement vector. The electric field components are related to the electric potential $\phi(x, z)$ by

$$E_x = -\phi_{,x}, \quad E_z = -\phi_{,z}. \tag{6}$$

With Eqs. (3)–(6), the governing equations become

$$\begin{aligned} &c_{11}u_{x,xx} + c_{44}u_{x,zz} + (c_{13} + c_{44})u_{z,xz} + (e_{31} + e_{15})\phi_{,xz} = 0, \\ &c_{44}u_{z,xx} + c_{33}u_{z,zz} + (c_{13} + c_{44})u_{x,xz} + e_{15}\phi_{,xx} + e_{33}\phi_{,zz} = 0, \end{aligned} \tag{7}$$

$$(e_{31} + e_{15})u_{x,xz} + e_{15}u_{z,xx} + e_{33}u_{z,zz} - \epsilon_{11}\phi_{,xx} - \epsilon_{33}\phi_{,zz} = 0. \tag{8}$$

In a vacuum, the constitutive Eq. (4) and the governing Eq. (8) become

$$D_x = \epsilon_0 E_x, \quad D_z = \epsilon_0 E_z, \tag{9}$$

$$\phi_{,xx} + \phi_{,zz} = 0 \tag{10}$$

where $\epsilon_0 = 8.85 \times 10^{-12}$ C/Vm is the dielectric permittivity of the vacuum.

We first consider the case 1 (see Fig. 1a). The permeable crack model is treated, and the boundary conditions at $z = 0$ are

$$\sigma_{zx}(x, 0) = 0 \quad (0 \le x \le h), \tag{11}$$

$$\left.\begin{aligned} &\sigma_{zz}(x, 0) = 0 \quad (0 \le x < a) \\ &u_z(x, 0) = 0 \quad (a \le x \le h) \end{aligned}\right\} \tag{12}$$

$$\left.\begin{aligned} &E_x(x, 0) = E_x^c(x, 0) \quad (0 \le x < a) \\ &\phi(x, 0) = 0 \qquad\qquad (a \le x \le h) \end{aligned}\right\} \tag{13}$$

$$D_z(x, 0) = D_z^c(x, 0) \quad (0 \le x < a) \tag{14}$$

where the superscript c stands for the electric field quantity in the void inside the crack. The electric potentials $\phi(x, z)$ and $\phi^c(x, z)$ and electric field intensities $E_x(x, z)$ and $E_x^c(x, z)$ are odd functions of z. The electric field intensity $E_x^c(x, 0)$ is zero on the symmetry plane inside the crack, and $E_x(x, 0)$ is equal to zero ahead of the crack, so the boundary conditions of Eq. (13) reduce to $E_x(x, 0) = 0$ $(0 \le x \le h)$. The condition $E_x(x, 0) = 0$ $(0 \le x \le h)$ is equivalent to the condition $\phi(x, 0) = 0$ $(0 \le x \le h)$. The loading conditions can be written as

$$u_z(x, l) = u_0, \quad \phi(x, l) = \phi_0 \quad (0 \le x \le h), \tag{15}$$

$$\sigma_{xx}(0, z) = 0, \quad \sigma_{xz}(0, z) = 0, \quad D_x(0, z) = 0 \quad (0 \le z \le l), \tag{16}$$

$$\sigma_{xx}(h, z) = 0, \quad \sigma_{xz}(h, z) = 0, \quad D_x(h, z) = 0 \quad (0 \le z \le l) \tag{17}$$

where u_0 is the applied displacement and ϕ_0 is the applied electric potential. In electrostatics, at a surface separating two dielectric media, the normal component of the electric displacement and the tangential component of the electric field are continuous. However, when one of the media is air, these two conditions can be approximated simply by one, namely that the normal component of the electric displacement vanishes at the surface. So the third of Eqs. (16), (17) is adopted here. This assumption is based on the fact that there is a very large difference between the dielectric constants of the piezoelectric material and the air [15]. The electric displacement $D_z(x, 0)$ is solved under the crack face boundary (Eqs. (11)–(13)) and loading (Eqs. (15)–(17)) conditions by the finite element analysis, and $D_z^c(x, 0)$ is determined by Eq. (14) precisely.

On the other hand, the impermeable boundary condition is given by

$$\left.\begin{array}{l} D_z(x,0) = 0 \quad (0 \le x < a) \\ \phi(x,0) = 0 \quad (a \le x \le h) \end{array}\right\}. \tag{18}$$

Also, the electrical boundary condition for the open crack model becomes

$$\left.\begin{array}{l} D_z^+ = D_z^- \quad (0 \le x < a) \\ D_z^+(u_z^+ - u_z^-) = \epsilon_0(\phi^- - \phi^+) \quad (0 \le x < a) \\ \phi(x,0) = 0 \quad (a \le x \le h) \end{array}\right\} \tag{19}$$

where the superscripts + and − denote the upper and lower crack faces, respectively.

By applying the loading conditions (15), the stress σ_{zz} for the uncracked piezoelectric material is obtained as

$$\sigma_{zz}(x, z) = \sigma_0 - e_1 E_0 \tag{20}$$

where

$$\sigma_0 = \left(c_{33} - \frac{c_{13}^2}{c_{11}}\right)\varepsilon_0, \tag{21}$$

$$\varepsilon_0 = \frac{u_0}{l}, \quad E_0 = -\frac{\phi_0}{l} \tag{22}$$

and

$$e_1 = e_{33} - \left(\frac{c_{13}}{c_{11}}\right)e_{31}. \tag{23}$$

The stress at $z = l$ for the uncracked piezoelectric material is denoted by $\sigma_l = \sigma_0 - e_1 E_0$. Note that σ_0 is the stress for a closed-circuit condition with the potential forced to remain zero (grounded) and depends only on the displacement at the edge $z = l$. When a uniform displacement u_0 is applied and fixed at $z = l$, the stress σ_0 will be uniform. On the other hand, when the stress σ_l is applied and fixed at $z = l$, σ_l is left unchanged and the displacement u_0 depends on E_0.

Next, we consider case 2 (see Fig. 1b). The boundary conditions at $x = 0$ are

$$\sigma_{xz}(0, z) = 0 \quad (0 \le z \le h), \tag{24}$$

$$\left.\begin{array}{l} \sigma_{xx}(0,z) = 0 \quad (0 \le z < a) \\ u_x(0,z) = 0 \quad (a \le z \le h) \end{array}\right\}, \tag{25}$$

$$\left.\begin{array}{ll} E_z(0,z) = E_z^c(0,z) & (0 \le z < a) \\ \phi_{,x}(0,z) = 0 & (a \le z \le h) \end{array}\right\}, \quad \begin{array}{l} (26.1) \\ (26.2) \end{array}$$

$$D_x(0, z) = D_x^c(0, z) \quad (0 \le z < a). \tag{27}$$

The loading conditions can be expressed in the form

$$u_x(l, z) = u_0, \quad D_x(l, z) = 0 \quad (0 \le z \le h), \tag{28}$$

$$\sigma_{zz}(x, 0) = 0, \quad \sigma_{zx}(x, 0) = 0, \quad \phi(x, 0) = 0 \quad (0 \le x \le l), \tag{29.1–3}$$

$$\sigma_{zz}(x, h) = 0, \quad \sigma_{zx}(x, h) = 0, \quad \phi(x, h) = \phi_0 \quad (0 \le x \le l). \tag{30.1–3}$$

The electric field intensity $E_z(0, z) = -\phi_0/h$ is obtained from Eqs. (29.3), (30.3), and $E_z^c(0, z) = -\phi_0/h$ is determined from Eq. (26.1). The electric displacement $D_x(0, z)$ is calculated using the crack face boundary (Eqs. (24)–(26)) and loading (Eqs. (28)–(30)) conditions by the finite element analysis, and $D_x^c(0, z)$ is determined from Eq. (27) precisely. Equations (26) and (27) are the permeable boundary conditions. We also consider the electrical boundary conditions for the impermeable and open crack models.

By applying the loading conditions, the stress σ_{xx} for the uncracked piezoelectric material is obtained as

$$\sigma_{xx}(x, z) = c_{11}\varepsilon_0. \tag{31}$$

The stress at $x = l$ for the uncracked piezoelectric material is denoted by $\sigma_l = c_{11}\varepsilon_0$ and is independent of the applied electric field $E_0 = -\phi_0/h$.

2.2 Polarization switching

A nonlinear finite element model incorporating the polarization switching mechanisms is presented. Two criteria are used. The first criterion (work done switching criterion) requires that a polarization switches when the combined electrical and mechanical work exceeds a critical value [16], i.e.,

$$\sigma_{xx}\Delta\varepsilon_{xx} + \sigma_{zz}\Delta\varepsilon_{zz} + 2\sigma_{zx}\Delta\varepsilon_{zx} + E_x\Delta P_x + E_z\Delta P_z \geq 2P^{\mathrm{s}}E_{\mathrm{c}} \tag{32}$$

where $\Delta\varepsilon_{xx}$, $\Delta\varepsilon_{zz}$, *and* $\Delta\varepsilon_{zx}$ are the changes in the spontaneous strain γ^{s}, ΔP_x and ΔP_z are the changes in the spontaneous polarization P^{s}, and E_{c} is a coercive electric field. It is assumed that the elastic and dielectric constants of the piezoelectric materials remain unchanged after 180° or 90° polarization switching, and only piezoelectric constants vary with switching. It is also assumed that for 90° switching there are two allowable directions of the poling in the coordinate system: in the positive and negative x-direction. This is due to the fact that the 90° switching in the yz plane does not impact the results. The changes in spontaneous strains and polarizations for 180° switching can be expressed as

$$\Delta\varepsilon_{xx} = \varepsilon_{xx}^{\mathrm{r}} = 0, \quad \Delta\varepsilon_{zz} = \varepsilon_{zz}^{\mathrm{r}} = 0, \quad \Delta\varepsilon_{zx} = \varepsilon_{zx}^{\mathrm{r}} = 0, \tag{33}$$

$$\Delta P_x = P_x^{\mathrm{r}} = 0, \quad \Delta P_z = P_z^{\mathrm{r}} = -2P^{\mathrm{s}}. \tag{34}$$

For 90° switching in the zx plane, there results

$$\Delta\varepsilon_{xx} = \varepsilon_{xx}^{\mathrm{r}} = \gamma^{\mathrm{s}}, \quad \Delta\varepsilon_{zz} = \varepsilon_{zz}^{\mathrm{r}} = -\gamma^{\mathrm{s}}, \quad \Delta\varepsilon_{zx} = \varepsilon_{zx}^{\mathrm{r}} = 0, \tag{35}$$

$$\Delta P_x = P_x^{\mathrm{r}} = \pm P^{\mathrm{s}}, \quad \Delta P_z = P_z^{\mathrm{r}} = -P^{\mathrm{s}}. \tag{36}$$

The second criterion (internal energy density criterion) is defined as [17]

$$U \geq U_{\mathrm{c}} \tag{37}$$

where U is the internal energy density and U_c is a critical value of internal energy density corresponding to the switching mode. The internal energy density associated with 180° switching can be written as

$$U = \frac{1}{2}D_z E_z. \tag{38}$$

In the case of 90° switching, the internal energy density is

$$U = \frac{1}{2}(\sigma_{xx}\varepsilon_{xx} + \sigma_{zz}\varepsilon_{zz} + 2\sigma_{zx}\varepsilon_{zx} + D_x E_x). \tag{39}$$

The critical value of internal energy density is assumed in the following form:

$$U_{\mathrm{c}} = \frac{1}{2}\epsilon_{33}^{\mathrm{T}}(E_{\mathrm{c}})^2 \tag{40}$$

where $\epsilon_{33}^{\mathrm{T}}$ is the dielectric permittivity at constant stress.

The constitutive Eqs. (3) and (4) after 180° switching are

$$\begin{Bmatrix} \sigma_{xx} \\ \sigma_{zz} \\ \sigma_{zx} \end{Bmatrix} = \begin{bmatrix} c_{11} & c_{13} & 0 \\ c_{13} & c_{33} & 0 \\ 0 & 0 & c_{44} \end{bmatrix} \begin{Bmatrix} \varepsilon_{xx} - \varepsilon_{xx}^{\mathrm{r}} \\ \varepsilon_{zz} - \varepsilon_{zz}^{\mathrm{r}} \\ 2(\varepsilon_{zx} - \varepsilon_{zx}^{\mathrm{r}}) \end{Bmatrix} + \begin{bmatrix} 0 & e_{31} \\ 0 & e_{33} \\ e_{15} & 0 \end{bmatrix} \begin{Bmatrix} E_x \\ E_z \end{Bmatrix}, \tag{41}$$

$$\begin{Bmatrix} D_x \\ D_z \end{Bmatrix} = -\begin{bmatrix} 0 & 0 & e_{15} \\ e_{31} & e_{33} & 0 \end{bmatrix} \begin{Bmatrix} \varepsilon_{xx} - \varepsilon_{xx}^{\mathrm{r}} \\ \varepsilon_{zz} - \varepsilon_{zz}^{\mathrm{r}} \\ 2(\varepsilon_{zx} - \varepsilon_{zx}^{\mathrm{r}}) \end{Bmatrix} + \begin{bmatrix} \epsilon_{11} & 0 \\ 0 & \epsilon_{33} \end{bmatrix} \begin{Bmatrix} E_x \\ E_z \end{Bmatrix} + \begin{Bmatrix} P_x^{\mathrm{r}} \\ P_z^{\mathrm{r}} \end{Bmatrix}. \tag{42}$$

The constitutive Eqs. (3) and (4) after 90° switching become

$$\begin{Bmatrix} \sigma_{xx} \\ \sigma_{zz} \\ \sigma_{zx} \end{Bmatrix} = \begin{bmatrix} c_{11} & c_{13} & 0 \\ c_{13} & c_{33} & 0 \\ 0 & 0 & c_{44} \end{bmatrix} \begin{Bmatrix} \varepsilon_{xx} - \varepsilon_{xx}^{\mathrm{r}} \\ \varepsilon_{zz} - \varepsilon_{zz}^{\mathrm{r}} \\ 2(\varepsilon_{zx} - \varepsilon_{zx}^{\mathrm{r}}) \end{Bmatrix} \mp \begin{bmatrix} e_{33} & 0 \\ e_{31} & 0 \\ 0 & e_{15} \end{bmatrix} \begin{Bmatrix} E_x \\ E_z \end{Bmatrix}, \tag{43}$$

$$\begin{Bmatrix} D_x \\ D_z \end{Bmatrix} = \pm\begin{bmatrix} e_{33} & e_{31} & 0 \\ 0 & 0 & e_{15} \end{bmatrix} \begin{Bmatrix} \varepsilon_{xx} - \varepsilon_{xx}^{\mathrm{r}} \\ \varepsilon_{zz} - \varepsilon_{zz}^{\mathrm{r}} \\ 2(\varepsilon_{zx} - \varepsilon_{zx}^{\mathrm{r}}) \end{Bmatrix} + \begin{bmatrix} 0 & \epsilon_{33} \\ \epsilon_{11} & 0 \end{bmatrix} \begin{Bmatrix} E_x \\ E_z \end{Bmatrix} + \begin{Bmatrix} P_x^{\mathrm{r}} \\ P_z^{\mathrm{r}} \end{Bmatrix}. \tag{44}$$

2.3 Dielectric breakdown

For the piezoelectric ceramics under high-positive electric fields, the material will break down electrically. A very simple model is used here for such electrical discharges. It is assumed that the material cannot support electric fields larger than the breakdown strength E_d [13]. That is, the electric field in the dielectric breakdown region is equal to E_d.

2.4 Energy release rate

The energy release rate G for the piezoelectric materials can be obtained from the following J-integral [10]:

$$\begin{aligned} G = J = \left(\int_{\Gamma_0} - \int_{\Gamma_\mathrm{p}} \right) \{ & H n_x - (\sigma_{xx} u_{x,x} + \sigma_{zx} u_{z,x}) n_x - (\sigma_{zx} u_{x,x} + \sigma_{zz} u_{z,x}) n_z \\ & + D_x E_x n_x + D_z E_x n_z \} d\Gamma \end{aligned} \tag{45}$$

where Γ_0 is a small contour closing a crack tip, Γ_p is a path embracing that part of phase boundary which is enclosed by Γ_0, and n_x and n_z are the components of the outer unit normal vector. The electrical enthalpy density H is

$$\begin{aligned} H = & \frac{1}{2}\{c_{11}(u_{x,x})^2 + c_{33}(u_{z,z})^2 + 2c_{13} u_{x,x} u_{z,z} + c_{44}(u_{x,z} + u_{z,x})^2\} \\ & - \frac{1}{2}\{\epsilon_{11}(E_x)^2 + \epsilon_{33}(E_z)^2\} \\ & - \{e_{15}(u_{x,z} + u_{z,x}) E_x + (e_{31} u_{x,x} + e_{33} u_{z,z}) E_z\}. \end{aligned} \tag{46}$$

The J-integrals for the permeable and impermeable crack models are path independent. If the crack gap can store energy, nonzero contributions to G for the open crack model arise from the contour segments along the crack face [18]. The values of G for the open crack model can be obtained by computing contour integrations and then subtracting the electrical enthalpy density of the crack gap H^c times the crack opening displacement evaluated at the intersection x^Γ of the contour with the crack faces [7]. So Eq. (45) becomes

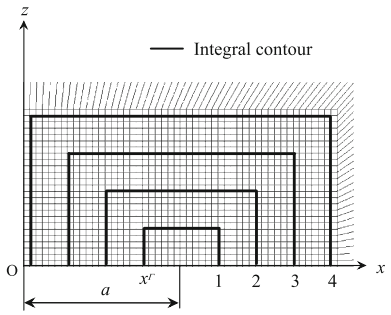

Fig. 2 Finite element mesh and boundaries of integration domains

Table 1 Material properties of PZTs

	Elastic stiffnesses ($\times 10^{10}$ N/m^2)				Piezoelectric coefficients (C/m^2)			Dielectric constants ($\times 10^{-10}$ C/Vm)	
	c_{11}	c_{33}	c_{44}	c_{13}	e_{31}	e_{33}	e_{15}	ϵ_{11}	ϵ_{33}
PCM-80	17.0	16.5	3.05	11.5	−5.99	15.6	13.7	95.2	68.4
C-91	12.0	11.4	2.4	7.7	−17.3	21.2	20.2	226	235

$$G = \left(\int_{\Gamma_0} - \int_{\Gamma_p} \right) \{ H n_x - (\sigma_{xx} u_{x,x} + \sigma_{zx} u_{z,x}) n_x - (\sigma_{zx} u_{x,x} + \sigma_{zz} u_{z,x}) n_z + D_x E_x n_x + D_z E_x n_z \} d\Gamma - 2H^c(x^\Gamma) u_z^+(x^\Gamma). \tag{47}$$

Note that the electrical traction $H^c + D_z^c E_z^c$ is accounted for on the crack faces in calculations in Eq. (47). The values of G for the nonlinear electrically discharging crack model can be obtained by using Eq. (47) and assuming that the crack gap behaves in a linear dielectric manner when the electric field within the crack gap is below a critical discharge level E_d^c [7].

A plane strain finite element analysis was carried out to evaluate the energy release rates for the permeable, impermeable, open, and discharging crack models using the domain integral method [19], and for the calculation of G, four domains were defined in the finite element mesh. Figure 2 gives the details of the crack tip mesh for Case 1. The G calculations for the open and discharging crack models are more complicated than for the permeable and impermeable crack models [20]. The Newton–Raphson method was used to find the solutions for the open and discharging crack models.

Each element consists of many grains, and each grain is modeled as a uniformly polarized cell that contains a single domain. The model neglects the domain wall effects and interaction among different domains. In reality, this is not true, but the assumption does not affect the macroscopic behavior of the cracked piezoelectric materials. The polarization of each grain initially aligns as closely as possible with the z-direction. The polarization switching is defined for each element. The displacement u_0 and electric potential ϕ_0 are applied, and the electromechanical fields of each element are computed from the finite element analysis. The switching criterion of Eq. (32) or (37) is checked for every element to see whether switching will occur. After all possible polarization switches have occurred, the piezoelectric tensor of each element is rotated to the new polarization direction, and the electromechanical fields are recalculated. Such a procedure is repeated until the evolution of the objective solutions shows no improvements. The possible occurrence of dielectric breakdown is also assessed for every element.

The spontaneous polarization P^s and strain γ^s are assigned representative values of 0.3 C/m^2 and 0.004, respectively. Our previous experiments [21,22] verified the accuracy of the above scheme and showed that the results obtained are of general applicability. After polarization switching or dielectric breakdown is predicted, integral paths are selected. The integral path does not pass exactly through the singular point.

3 Numerical results and discussion

Numerical calculations have been carried out for commercially available piezoelectric ceramics, hard PZT PCM-80 (Panasonic Electric Devices Co., Ltd., Japan) and soft PZT C-91 (Fuji Ceramics Co., Ltd., Japan).

Table 2 Energy release rate for rectangular piezoelectric material PCM-80 ($a = 1$ mm) under $u_0 = 1$ μm and $E_0 = 0.1$ MV/m (Case 1)

PCM-80 Case 1	G(N/m^2)			
	Permeable	Impermeable	Open	Discharging
Domain				
1	1.785	1.674	1.761 (-6.7×10^{-3})	1.785 (-7.8×10^{-6})
2	1.782	1.673	1.744 (-8.0×10^{-3})	1.781 (-9.3×10^{-6})
3	1.779	1.674	1.735 (-9.1×10^{-3})	1.779 (-1.1×10^{-5})
4	1.777	1.676	1.729 (-1.0×10^{-2})	1.777 (-1.2×10^{-5})
Avg.	1.781	1.674	1.742 (-8.5×10^{-3})	1.780 (-9.8×10^{-6})
Line				
1	1.785	1.674	1.768 (-6.7×10^{-3})	1.785 (-7.8×10^{-6})
2	1.778	1.672	1.752 (-9.3×10^{-3})	1.778 (-1.1×10^{-5})
3	1.775	1.677	1.744 (-1.1×10^{-2})	1.774 (-1.3×10^{-5})
4	1.772	1.681	1.739 (-1.3×10^{-2})	1.771 (-1.5×10^{-5})
Avg.	1.777	1.676	1.751 (-1.0×10^{-2})	1.777 (-1.2×10^{-5})

Values in parentheses are the results of $2H^c(x^\Gamma)u_z^+(x^\Gamma)$ in Eq. (47)

The material properties are listed in Table 1, and the coercive electric fields of PCM-80 and C-91 are approximately $E_c = 2$ and 0.35 MV/m, respectively. The crack length a is varied while keeping the ceramic width and length at $h = 10$ and $2l = 20$ mm, respectively. For the calculations of the energy release rate for the discharging crack model, the standard air breakdown field $E_d^c = 3$ MV/m is used. Also, the breakdown strength of PZT ceramics is assumed as $E_d = 10$ MV/m [23] to predict the dielectric breakdown.

We first consider the cracked piezoelectric ceramics under applied displacement. Table 2 lists the energy release rate for the permeable, impermeable, open, and discharging crack models for the rectangular piezoelectric material PCM-80 ($a = 1$ mm) under displacement $u_0 = 1$ μm and electric field $E_0 = 0.1$ MV/m (Case 1). The results obtained by the four domains and the average values (Avg.) are shown, and the values in parentheses are the contribution from the crack interior (see Eq. 47). Also shown are the results determined from the line integral method. The error is reasonable and not important here from the practical point of view. It is found that for the open and discharging crack models the contribution from the crack interior is negligible under practical loading conditions. Also, the values of $2H^c(x^\Gamma)u_z^+(x^\Gamma)$ for the discharging crack model are significantly smaller than those for the open crack model. In addition, it is interesting to note that the energy release rates predicted by the permeable and discharging crack models are not significantly different. From the table, it is clear that the values determined from the domain and line integral methods are in good agreement. Average G values from the domain integral method are presented in the following Figures.

Figure 3 shows the dependence of the energy release rate G for the permeable, impermeable, open, and discharging crack models on the electric field E_0 in the rectangular piezoelectric material PCM-80 under the displacement $u_0 = 1$ μm for $a = 1$ and 2.5 mm (Case 1). Note that small differences are observed between the permeable (solid line) and discharging (dot-dashed line) crack models under various electric fields. The energy release rate G under an applied displacement decreases with increasing positive electric fields. A negative energy release rate can be induced with positive electric fields in the impermeable and open crack models. According to the fracture mechanics interpretation, a negative energy release rate would correspond to a crack that could absorb energy due to crack extension. Since this would exclude the fracture in piezoelectric ceramics under electric fields, the parameters for the impermeable and open crack models have questionable physical significance. It is therefore clear that the impermeable and open crack models are not appropriate for a slit crack in piezoelectric ceramics. Figure 4 summarizes the results for the permeable, impermeable, open, and discharging cracks normal and parallel to the poling (electric field) and shows the energy release rate G versus the electric field E_0 for the rectangular piezoelectric material PCM-80 under $u_0 = 1$ μm for $a = 1$ mm (Cases 1 and 2). For the piezoelectric material with a crack parallel to the poling and electric field, no difference is observed among the four crack models, and the energy release rate is independent of the electric field (see Case 2). Hence, the piezoelectric crack normal to the poling and electric field is important.

Figure 5 displays the variation of the energy release rate G with the negative electric field E_0 for the permeable crack model ($a = 1$ mm) in the rectangular piezoelectric material PCM-80 under $u_0 = 0.1$ μm (Case 1), predicted by the criteria based on the work (32) and energy density (37). Also shown is the result without switching effect. The prediction by the criterion based on the work shows that polarization switching leads to a

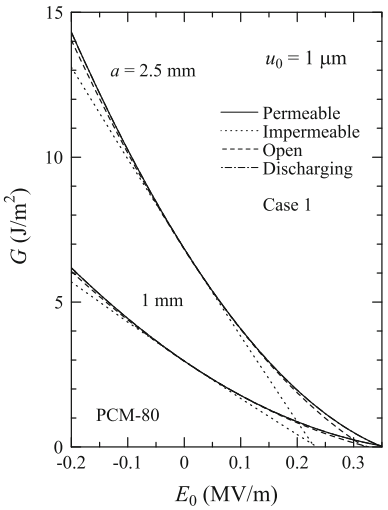

Fig. 3 Energy release rate versus electric field under the displacement $u_0 = 1$ μm (PCM-80, Case 1)

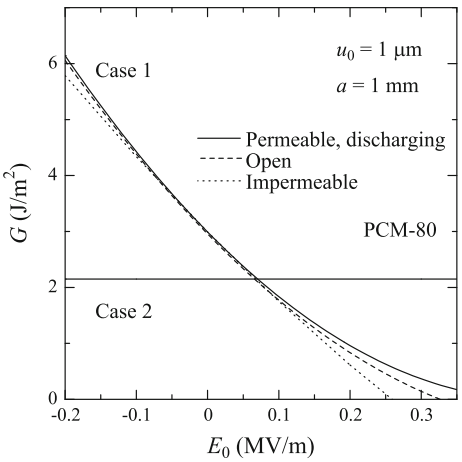

Fig. 4 Energy release rate versus electric field under the displacement $u_0 = 1$ μm (PCM-80, Cases 1 and 2)

sudden decrease in G after E_0 reaches about -1.93 MV/m. When E_0 reaches -2 MV/m (the coercive electric field), G has reached about 5 J/m^2 (minimum value). As the field is reduced below -2 MV/m, G is increased. On the other hand, the prediction according to the energy density shows that the value of G deviates gradually from the result without switching effect. As E_0 is reduced below -2.05 MV/m, G is decreased. The same results are obtained for the discharging crack model (not shown). It is expected from the figure that the hard PZT PCM-80 ceramics will fail under a negative electric field before the polarization switching. This is due to the fact that the critical energy release rate for the PZT PCM-80 is about 10 J/m^2 [24]. Figure 6 shows the similar results for the rectangular piezoelectric material C-91. The prediction based on the work shows that polarization switching leads to a sudden decrease in G after E_0 reaches about -0.33 MV/m. When the negative electric field increases further, G again increases reaching a peak and then decreases. When E_0 reaches -0.35 MV/m (the coercive electric field), G has reached about 0 J/m^2 (minimum value). On the other hand, the energy density criterion shows that the value of G deviates gradually from the result without switching effect. It is expected that the nonlinear effect caused by the polarization switching will affect the crack behavior in the soft PZT C-91 ceramics. Figure 7 shows the 180° and 90° switching zones near the permeable crack tip ($a = 1$ mm) in the C-91 under $u_0 = 0.1$ μm for $E_0 = -0.31, -0.34$ MV/m (Case 1), predicted by the criteria based on the (a) work and (b) energy density. The work criterion shows that only the 180° switching occurs near the crack tip under high-negative electric field. If the criterion based on the energy density is used, the region near the crack tip is found to undergo 90° switching. Figure 8 shows similar results for $a = 5$ mm. The switching zones depend on the crack length.

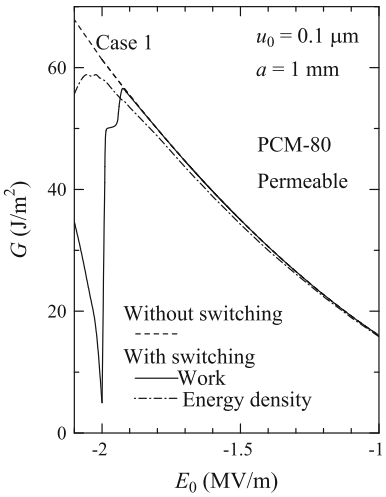

Fig. 5 Energy release rate versus negative electric field under the displacement $u_0 = 0.1$ μm (PCM-80, Case 1)

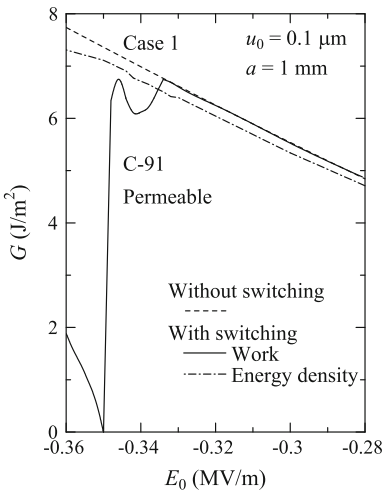

Fig. 6 Energy release rate versus negative electric field under the displacement $u_0 = 0.1$ μm (C-91, Case 1)

Next, we discuss the cracked piezoelectric ceramics under applied stress. Figure 9 shows the energy release rate G versus the electric field E_0 of the permeable, impermeable, open, and discharging crack models for $a = 1$ mm in the rectangular piezoelectric material PCM-80 under stress $\sigma_l = 8$ MPa (Case 1), corresponding to the uniform displacement $u_0 = 1$ μm for the uncracked material without the electric field. The switching criteria are not considered. The energy release rates for the permeable and discharging crack models are independent of the electric field. Figure 10 displays the variation of G with negative electric field E_0 of the permeable crack model ($a = 1$ mm) for the same material and conditions with and without polarization switching effect. For the switching effect, the predictions by the criteria based on work (Eq. (32)) and energy density (Eq. (37)) are shown. The behavior of the energy release rate in the negative E_0 is complicated because of the polarization switching phenomena. When the negative E_0 increases, G predicted by the work and energy density becomes larger and smaller than that without the switching effect, respectively. The work criterion indicates that the switching causes an anti-shielding effect. The experimental work [25] showed that the crack length of PZT ceramics under load deviates from the linear function of the electric field, especially for negative electric fields. That is, the polarization switching could produce additional crack growth. By including the polarization switching effect of the energy release rate, the observed nonlinear dependence of the piezoelectric crack behavior on the electric field is explained. The 180° switching just above the crack face decreases G, and extensive 180° switching ahead of the crack tip, based on the work, leads to an increase in G (see Fig. 11). The 90° switching does not occur in PCM-80. Figure 12 shows G versus negative E_0 for C-91, corresponding to Fig. 10. The value of the electric field associated with the switching is -0.34 MV/m for the criterion based on

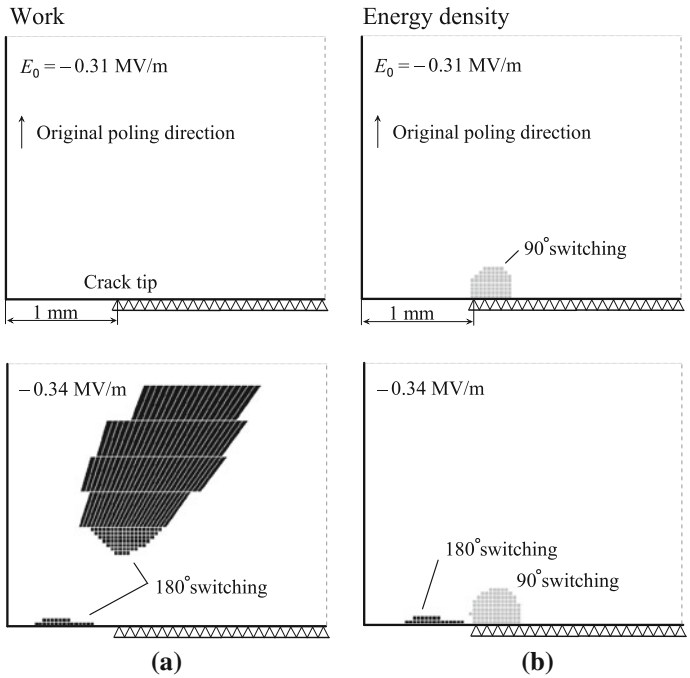

Fig. 7 Polarization switching zone near the permeable crack ($a = 1$mm) induced by displacement $u_0 = 0.1\,\mu$m and electric fields $E_0 = -0.31, -0.34$ MV/m based on different criteria: **a** work and **b** energy density (C-91, Case 1)

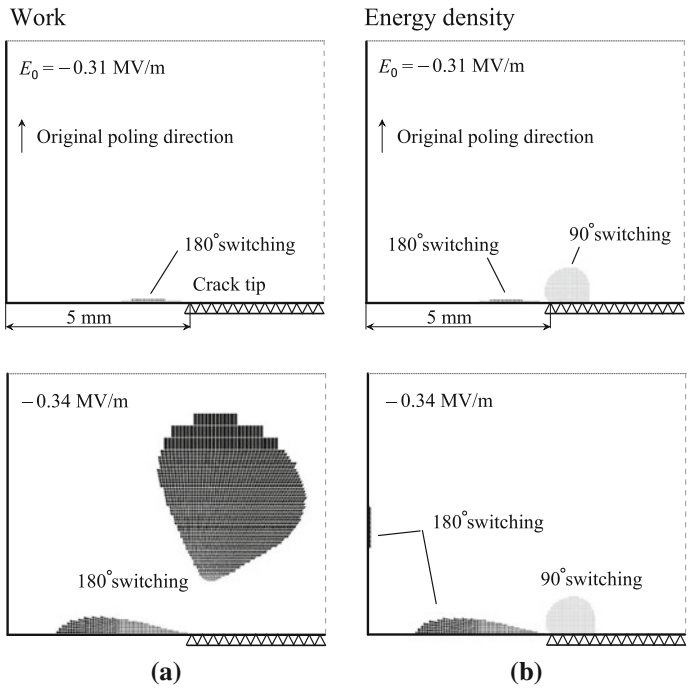

Fig. 8 Polarization switching zone near the permeable crack ($a = 5$ mm) induced by displacement $u_0 = 0.1\,\mu$m and electric fields $E_0 = -0.31, -0.34$ MV/m based on different criteria: **a** work and **b** energy density (C-91, Case 1)

the work while it is approximately -0.2 MV/m (not shown) for the criterion based on the energy density. The 90° switching near the crack tip, based on the energy density, leads to a small decrease in G (see Fig. 13). The above results show that if the piezoelectric ceramics are operated under negative electric fields, the polarization switching effect is by no means negligible, and the designers need to be aware of nonlinear behavior.

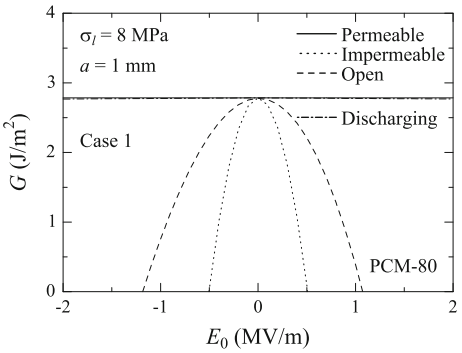

Fig. 9 Energy release rate versus electric field under the stress $\sigma_l = 8$ MPa (PCM-80, Case 1)

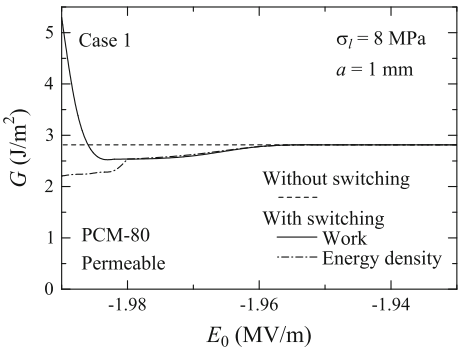

Fig. 10 Energy release rate versus negative electric field under the stress $\sigma_l = 8$ MPa (PCM-80, Case 1)

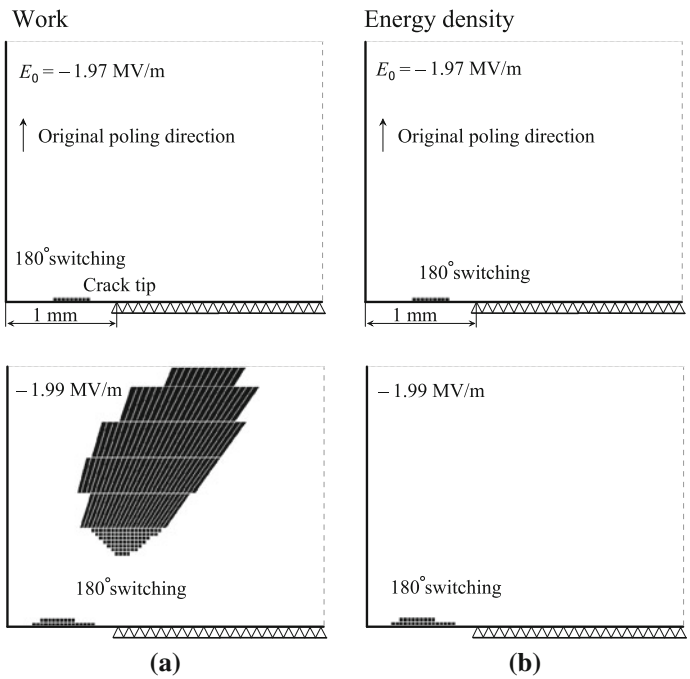

Fig. 11 Polarization switching zone near the permeable crack ($a = 1$ mm) induced by stress $\sigma_l = 8$ MPa and electric fields $E_0 = -1.97, -1.99$ MV/m based on different criteria: **a** work and **b** energy density (PCM-80, Case 1)

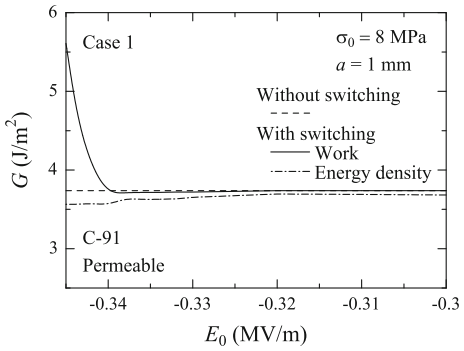

Fig. 12 Energy release rate versus negative electric field under the stress $\sigma_l = 8$ MPa (C-91, Case 1)

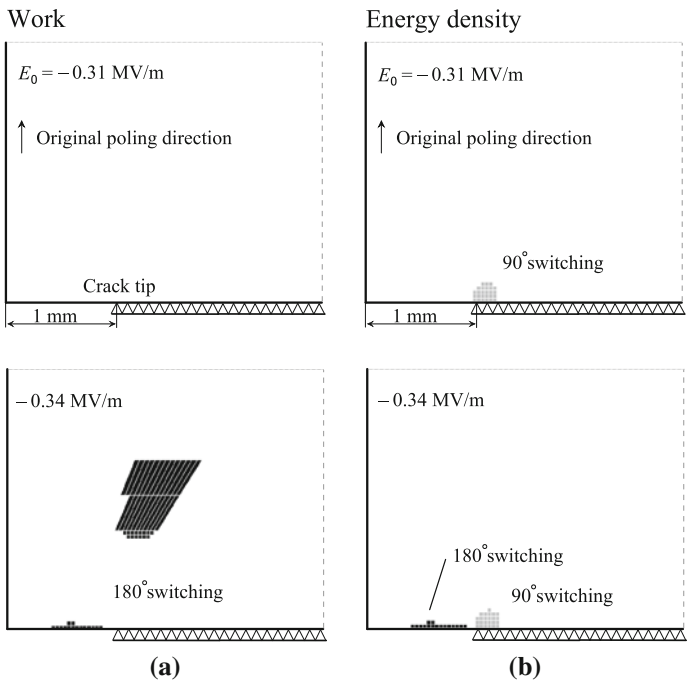

Fig. 13 Polarization switching zone near the permeable crack ($a = 1$ mm) induced by stress $\sigma_l = 8$ MPa and electric fields $E_0 = -0.31, -0.34$ MV/m based on different criteria: **a** work and **b** energy density (C-91, Case 1)

Figure 14 shows the predicted dielectric breakdown regions near the (a) permeable and (b) impermeable crack tip for the rectangular piezoelectric material PCM-80 ($a = 1$ mm) under stress $\sigma_l = 8$ MPa and various high-positive electric fields (Case 1). In the case of the permeable crack model, the dielectric breakdown does not occur under a high-positive electric field. On the other hand, the dielectric breakdown region increases with an increase in the positive electric field for the impermeable crack model. However, the energy release rate for the impermeable crack model under a high-positive electric field is negative (see Fig. 9); hence, the predicted region is meaningless. Similar phenomena are also shown for the rectangular piezoelectric material C-91 (no Figure shown). Although some previous works dealt with the dielectric breakdown model in cracked piezoelectric ceramics, we recommend the use of an exact piezoelectric crack model and practical loading conditions.

4 Conclusions

A finite element analysis was presented for the piezoelectric materials with a single-edge crack under tension. It was shown that the crack normal to the poling and electric field is important to investigate the piezoelectric

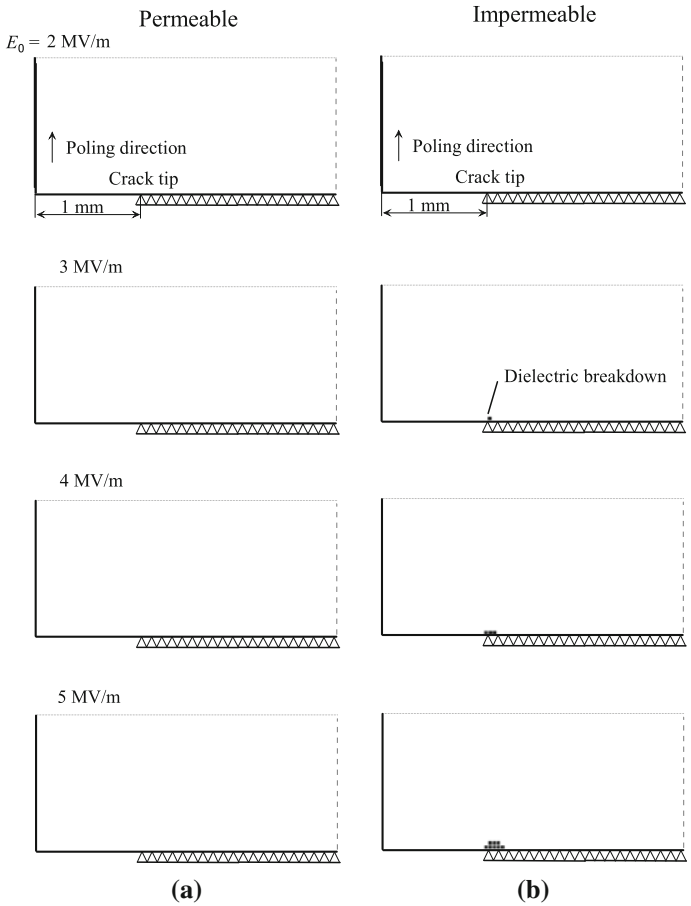

Fig. 14 Dielectric breakdown region near the **a** permeable and **b** impermeable crack ($a = 1$ mm) induced by stress $\sigma_l = 8$ MPa and electric fields $E_0 = 2, 3, 4, 5$ MV/m (PCM-80, Case 1)

fracture mechanics parameters such as the energy release rate. Based on the results of this study, the following conclusions may be inferred:

(i) Piezoelectric crack face boundary conditions strongly affect the electric field effect characteristics of the energy release rate. The energy release rate criteria for the open and impermeable crack models lead to negative values, which mean a crack that absorbs energy due to crack extension. On the other hand, the energy release rates for the permeable and discharging crack models are identical and always remain positive.

(ii) If a negative electric field is applied, localized polarization switching occurs due to electromechanical field concentrations near the crack tip, and the switching causes a sudden change in the energy release rate.

(iii) If a high-positive electric field is applied, dielectric breakdown occurs near the impermeable crack tip. However, the breakdown does not occur near the permeable crack tip. Different crack models give different results for the dielectric breakdown.

References

1. Parton, V.Z.: Fracture mechanics of piezoelectric materials. Acta Astro. **3**, 671–683 (1976)
2. Shindo, Y., Ozawa, E., Nowacki, J.P.: Singular stress and electric fields of a cracked piezoelectric strip. Int. J. Appl. Electromagn. Mater. **1**, 77–87 (1990)
3. Sosa, H.A.: On the fracture mechanics of piezoelectric solids. Int. J. Solids Struct. **29**, 2613–2622 (1992)
4. Pak, Y.E.: Linear electro-elastic fracture mechanics of piezoelectric materials. Int. J. Fract. **54**, 79–100 (1992)
5. Hao, T.-H., Shen, Z.-Y.: A new electric boundary condition of electric fracture mechanics and its applications. Eng. Fract. Mech. **47**, 793–802 (1994)

6. Zhao, M.H., Xu, G., Fan, C.Y.: Hybrid extended displacement discontinuity-charge simulation method for analysis of cracks in 2D piezoelectric media. Eng. Anal. Bound. Elem. **33**, 592–600 (2009)
7. Landis, C.M.: Energetically consistent boundary conditions for electromechanical fracture. Int. J. Solids Struct. **41**, 6291–6315 (2004)
8. Shindo, Y., Narita, F., Hirama, M.: Effect of the electrical boundary condition at the crack face on the mode I energy release rate in piezoelectric ceramics. Appl. Phys. Lett. **94**, 081902 (2009)
9. Fang, D.N., Sun, C.T. : Experimental study of fatigue and fracture of piezoceramics. In: Shindo, Y. (ed.) Mechanics of Electromagnetic Material Systems and Structures, pp. 103–114. WIT Press, Boston (2003)
10. Shindo, Y., Narita, F., Mikami, M.: Double torsion testing and finite element analysis for determining the electric fracture properties of piezoelectric ceramics. J. Appl. Phys. **97**, 114109 (2005)
11. Shindo, Y., Narita, F., Horiguchi, K., Magara, Y., Yoshida, M.: Electric fracture and polarization switching properties of piezoelectric ceramic PZT studied by the modified small punch test. Acta Mater. **51**, 4773–4782 (2003)
12. Gao, H., Zhang, T.-Y., Tong, P.: Local and global energy release rates for an electrically yielded crack in a piezoelectric ceramic. J. Mech. Phys. Solids **45**, 491–510 (1997)
13. Zhang, T.-Y., Zhao, M.-H., Gao, C.-F.: The strip dielectric breakdown model. Int. J. Eng. Sci. **132**, 311–327 (2005)
14. Fan, C.-Y., Zhao, M.-H., Zhou, Y.-H.: Numerical solution of polarization saturation/dielectric breakdown model in 2D finite piezoelectric media. J. Mech. Phys. Solids **57**, 1527–1544 (2009)
15. Narita, F., Shindo, Y., Horiguchi, K. : Electroelastic fracture mechanics of piezoelectric ceramics. In: Shindo, Y. (ed.) Mechanics of Electromagnetic Material Systems and Structures, pp. 89–101. WIT Press, Boston (2003)
16. Hwang, S.C., Lynch, C.S., McMeeking, R.M.: Ferroelectric/ferroelastic interactions and a polarization switching model. Acta Metall. Mater. **43**, 2073–2084 (1995)
17. Sun, C.T., Achuthan, A.: Domain-switching criteria for ferroelectric materials subjected to electrical and mechanical loads. J. Am. Ceram. Soc. **87**, 395–400 (2004)
18. McMeeking, R.M.: The energy release rate for a Griffith crack in a piezoelectric material. Eng. Fract. Mech. **71**, 1149–1163 (2004)
19. Li, F.Z., Shih, C.F., Needleman, A.: A comparison of methods for calculating energy release rates. Eng. Fract. Mech. **21**, 405–421 (1985)
20. McMeeking, R.M.: Crack tip energy release rate for a piezoelectric compact tension specimen. Eng. Fract. Mech. **64**, 217–244 (1999)
21. Shindo, Y., Yoshida, M., Narita, F., Horiguchi, K.: Electroelastic field concentrations ahead of electrodes in multilayer piezoelectric actuators: experiment and finite element simulation. J. Mech. Phys. Solids **52**, 1109–1124 (2004)
22. Narita, F., Shindo, Y., Hayashi, K.: Bending and polarization switching of piezoelectric laminated actuators under electromechanical loading. Comput. Struct. **83**, 1164–1170 (2005)
23. Tani, T., Asai, M., Takatori, K., Kamiya, N.: Evaluation of dielectric strength and breakdown behavior for Sr-, Nb-doped PZT ceramics with various shapes of electrodes. J. Ceram. Soc. Jap. **105**, 308–311 (1997)
24. Shindo, Y., Narita, F., Hirama, M.: Dynamic fatigue of cracked piezoelectric ceramics under electromechanical loading: three-point bending test and finite element analysis. J. Mech. Mater. Struct. **4**, 719–729 (2009)
25. Sun, C.T., Park, S.B.: Measuring fracture toughness of piezoceramics by Vickers indentation under the influence of electric fields. Ferroelectrics **248**, 79–95 (2000)